ESC European Society of Cardiology

Cardiovascular Research (2019) **115**, 1986–1997
doi:10.1093/cvr/cvz111

Altered C10 domain in cardiac myosin binding protein-C results in hypertrophic cardiomyopathy

Diederik W.D. Kuster [1,2†], Thomas L. Lynch IV [1†], David Y. Barefield [1,3], Mayandi Sivaguru[4], Gina Kuffel [5], Michael J. Zilliox [5], Kyoung Hwan Lee [6], Roger Craig[6], Rajasekaran Namakkal-Soorappan[7], and Sakthivel Sadayappan [1,8*]

[1]Cell and Molecular Physiology, Loyola University Chicago, Maywood, IL, USA; [2]Department of Physiology, Amsterdam UMC, Vrije Universiteit Amsterdam, Amsterdam Cardiovascular Sciences, Amsterdam, Netherlands; [3]Center for Genetic Medicine, Northwestern University, Chicago, IL, USA; [4]Institute for Genomic Biology, University of Illinois at Urbana-Champaign, Champaign, IL, USA; [5]Public Health Sciences, Loyola University Chicago, Maywood, IL, USA; [6]Division of Cell Biology and Imaging, Department of Radiology, University of Massachusetts Medical School, Worcester, MA, USA; [7]Molecular and Cellular Pathology, Department of Pathology, School of Medicine, The University of Alabama at Birmingham, Birmingham, AL, USA; and [8]Heart, Lung and Vascular Institute, Division of Cardiovascular Health and Disease, Department of Internal Medicine, University of Cincinnati, 231 Albert Sabin Way, Cincinnati, OH 45267-0575, USA

Received 20 December 2018; revised 4 April 2019; editorial decision 17 April 2019; accepted 25 April 2019; online publish-ahead-of-print 3 May 2019

Time for primary review: 32 days

Aims A 25-base pair deletion in the cardiac myosin binding protein-C (cMyBP-C) gene (*MYBPC3*), proposed to skip exon 33, modifies the C10 domain (cMyBP-C$^{\Delta C10mut}$) and is associated with hypertrophic cardiomyopathy (HCM) and heart failure, affecting approximately 100 million South Asians. However, the molecular mechanisms underlying the pathogenicity of cMyBP-C$^{\Delta C10mut}$ *in vivo* are unknown. We hypothesized that expression of cMyBP-C$^{\Delta C10mut}$ exerts a poison polypeptide effect leading to improper assembly of cardiac sarcomeres and the development of HCM.

Methods and results To determine whether expression of cMyBP-C$^{\Delta C10mut}$ is sufficient to cause HCM and contractile dysfunction *in vivo*, we generated transgenic (TG) mice having cardiac-specific protein expression of cMyBP-C$^{\Delta C10mut}$ at approximately half the level of endogenous cMyBP-C. At 12 weeks of age, significant hypertrophy was observed in TG mice expressing cMyBP-C$^{\Delta C10mut}$ (heart weight/body weight ratio: 4.43 ± 0.11 mg/g non-transgenic (NTG) vs. 5.34 ± 0.25 mg/g cMyBP-C$^{\Delta C10mut}$, $P < 0.05$). Furthermore, haematoxylin and eosin, Masson's trichrome staining, as well as second-harmonic generation imaging revealed the presence of significant fibrosis and a greater relative nuclear area in cMyBP-C$^{\Delta C10mut}$ hearts compared with NTG controls. M-mode echocardiography analysis revealed hypercontractile hearts (EF: 53.4%±2.9% NTG vs. 66.4% ± 4.7% cMyBP-C$^{\Delta C10mut}$; $P < 0.05$) and early diastolic dysfunction (E/E': 28.7 ± 3.7 NTG vs. 46.3 ± 8.4 cMyBP-C$^{\Delta C10mut}$; $P < 0.05$), indicating the presence of an HCM phenotype. To assess whether these changes manifested at the myofilament level, contractile function of single skinned cardiomyocytes was measured. Preserved maximum force generation and increased Ca^{2+}-sensitivity of force generation were observed in cardiomyocytes from cMyBP-C$^{\Delta C10mut}$ mice compared with NTG controls (EC_{50}: 3.6 ± 0.02 μM NTG vs. 2.90 ± 0.01 μM cMyBP-C$^{\Delta C10mut}$; $P < 0.0001$).

Conclusion Expression of cMyBP-C protein with a modified C10 domain is sufficient to cause contractile dysfunction and HCM *in vivo*.

Keywords Cardiac myosin binding protein-C • Diastolic dysfunction • Fibrosis • Transgenic mouse model • South Asian population

1. Introduction

Hypertrophic cardiomyopathy (HCM) is a genetic heart disease affecting one in 200–500 people.[1] HCM is clinically defined by left ventricular (LV) hypertrophy (mainly affecting the septal wall), diastolic dysfunction, mitral valve regurgitation, abnormal coronary microcirculatory function, and electrocardiographic abnormalities.[2] The aetiology of HCM stems from mutations in genes encoding cardiac contractile proteins, in

* Corresponding author. Tel: +1 513 558 7498; fax: +1 513-558-2884, E-mail: sadayasl@ucmail.uc.edu

† The first two authors contributed equally to the study.

particular mutations in *MYBPC3*, encoding cardiac myosin binding protein-C (cMyBP-C), as the most common origin of disease pathogenesis.[3] Evidence suggests that a subset of these mutations can cause an increase of toxic mutant and truncated proteins that leads to proteotoxicity in the heart owing to either specific interactions of the mutant protein or general misfolding that can cause cellular dysfunction and contribute to the development of HCM.[4–7] In cases of mutations that cause misfolded protein aggregates, it follows that targeting proteotoxicity would be a reasonable therapeutic approach to counteract the resultant proteopathy[6,8–10] by removing the offending truncated sarcomeric proteins.[6,11–13] However, the aetiology that would explain why specific *MYBPC3* mutant proteins lead to disease is likely variable and remains poorly understood.

The first *MYBPC3* mutations associated with HCM were reported in 1995.[14,15] Since then, more than 350 mutations have been published for this gene,[16] with population-specific founder effects.[17–19] cMyBP-C is a key sarcomeric thick-filament protein that interacts with both myosin and actin filaments to regulate sarcomere structure and function.[20] Importantly, 70% of all *MYBPC3* mutations include premature stop codons or frame shifts that encode proteins lacking key myosin binding residues in the C-terminus, which prevents protein incorporation into the sarcomere.[21,22] The pathogenic mechanism of *MYBPC3* mutations could stem from either an insufficient amount of gene product and, hence, reduced sarcomeric cMyBP-C, i.e. haploinsufficiency, direct pathogenic effects of the mutants on normal myofilament function, i.e. a poison polypeptide effect, or an accumulation of misfolded proteins, i.e. proteotoxicity.[23–29] Studying the specific pathogenic mechanism for specific *MYBPC3* mutations is confounded by an incomplete penetrance and variable onset of these mutations, which can be exacerbated by other physical or genetic modifiers,[26,30] suggesting that several factors may be involved in the prognosis of HCM. Therefore, it is important to determine the pathogenicity and underlying molecular mechanism(s) of each mutation in the context of HCM as an essential first step in identifying targets for therapies directed towards sarcomeric cardiomyopathies.[31,32]

Previously, we discovered a specific variant in *MYBPC3*, a 25-base pair deletion that leads to the loss of the splicing branch point in intron 32.[19,21,33,34] This variant affects approximately 100 million South Asians and is associated with HCM and heart failure (HF).[19,35,36] This mutation is thought to result in the skipping of exon 33 with a corresponding replacement of 62 amino acids with 55 non-native amino acids at the C10 domain of the C-terminus of cMyBP-C (cMyBP-C$^{\Delta C10mut}$).[21] The mutation was found to be associated with the development of HCM and HF.[19] Individuals carrying this variant are at high risk of developing HCM, but its functional and molecular effects are largely unknown.[19] Adenoviral expression of cMyBP-C$^{\Delta C10mut}$ in adult rat cardiomyocytes showed contractile dysfunction,[37] but whether expression of cMyBP-C$^{\Delta C10mut}$ alone is enough to cause an HCM phenotype *in vivo* remains elusive. Similar *MYBPC3* mutations have been shown to be quickly degraded; however, we have recently identified an additional mutation, D389V, which occurs in a subpopulation of cMyBP-C$^{\Delta C10mut}$ carriers.[38] This D389V variant occurs on the same allele as the cMyBP-C$^{\Delta C10mut}$ and is strongly associated with a HCM phenotype, suggesting that this protein is present in appreciable levels to cause dysfunction.

Therefore, to study the pathogenic potential of the cMyBP-C$^{\Delta C10mut}$ mutation *in vivo*, we generated transgenic (TG) mice expressing cardiac-specific cMyBP-C$^{\Delta C10mut}$ to define the link between cMyBP-C$^{\Delta C10mut}$ expression and HCM. We found that cMyBP-C$^{\Delta C10mut}$ did not incorporate into the C-zone of the sarcomere, but rather localized to the cytosol and Z-line. This evidence supports the poison-polypeptide hypothesis, in which an increase of toxic mutant and truncated proteins leads to a cascade of events beginning with improper incorporation of cMyBP-C$^{\Delta C10mut}$, then contractile dysfunction, and finally the induction of pro-hypertrophic signalling and cardiac remodelling. This study details the progressive pathogenicity of these events, thus providing mechanistic insight into the *in vivo* pathogenicity of the most common mutation associated with the development of HCM.

2. Methods

An expanded Methods section can be found in the Supplementary material online.

2.1 Cardiac-specific cMyBP-C$^{\Delta C10mut}$ transgenic mouse model

The previously generated mouse cMyBP-C wild-type cDNA (~3.8 kb) (Accession # NM_008653) was subjected to removal of exon 33, including 62 residues, and 55 non-native residues were introduced to generate the cMyBP-C$^{\Delta C10mut}$ protein.[37] The sequence encoding the myc epitope tag (10 amino acids, EQKLISEEDL, Roche) was incorporated into the primer such that the tag was placed after the initiator Met residue. The anti-Myc antibody was used to distinguish the cMyBP-C$^{\Delta C10mut}$ protein from endogenous cMyBP-C. After the correct sequence was confirmed, the entire cDNA fragment was ligated into the mouse *Myh6* promoter vector at the unique *SalI* site. The final construct was then resequenced to ensure the correct orientation. Next, the construct (~10 kb) was digested free of the vector sequence (~2.8 kb) with *NotI*, purified from agarose gels, and used to generate multiple TG lines (C57BL/6 strain). We obtained seven founder lines that were identified by PCR using primers corresponding to the α-MyHC 5'-untranslated (UTR) region with an internal control. An initial screening was performed on TG expression levels with a cMyc antibody (Data not shown), and the line with the highest levels of transgene expression was found and then selected for further analysis. All animal experiments were approved by the Institutional Animal Care and Use Committee at Loyola University Chicago and the University of Cincinnati and followed the policies described in the *Guide for the Use and Care of Laboratory Animals* published by the National Institutes of Health. Carbon dioxide (CO_2) inhalation was used for euthanasia via the chamber method. This method employs a top-opening chamber into which the animal(s) was/were introduced. After the animal(s) was/were placed in the chamber, a slow flow of CO_2 was initiated for a few minutes to slowly establish a high concentration at the bottom of the chamber. After breathing had stopped and the animal(s) were unconscious, euthanasia was completed by thoracotomy and removal of the heart for processing.

2.2 Mouse echocardiography

To assess cardiac function in non-transgenic (NTG) and cMyBP-C$^{\Delta C10mut}$ animals at 3 months of age, non-invasive M-mode echocardiography was performed using a VisualSonics Vevo 2100 imaging system (FUJIFILM VisualSonics Inc.) with an MS-550D 22–55 MHz transducer, as described previously.[39] Under isoflurane anaesthesia delivered via inhalation (5% for knockdown and 1.5% for sedation during the duration of the procedure), the hearts were monitored to assess function and morphology.

2.2 Histopathology

To assess gross morphology, cardiac sections were taken from NTG and cMyBP-C$^{\Delta C10mut}$ hearts and stained with haematoxylin and eosin (H&E) or Masson's trichrome (MT), as described previously.[39]

2.3 mRNA isolation, qPCR, and RNA-seq analysis

Gene expression changes between NTG and cMyBP-C$^{\Delta C10mut}$ hearts were evaluated as described previously.[39]

2.4 cMyBP-C$^{\Delta C10mut}$ protein localization analysis

To determine the localization of the cMyBP-C$^{\Delta C10mut}$ protein in the cardiac sarcomere of ΔC10 mice, cardiomyocytes were isolated from cMyBP-C$^{\Delta C10mut}$ hearts, as well as NTG hearts, for comparison. Following their isolation, cultured cardiomyocytes were fixed, permeabilized, and incubated with antibodies to detect endogenous cMyBP-C, myc-tagged cMyBP-C$^{\Delta C10mut}$ protein, and α-actinin.[37] The immunofluorescence-labelled cardiomyocytes from NTG and cMyBP-C$^{\Delta C10mut}$ hearts were imaged using a Leica TCS SP5 microscope.

2.5 Second-harmonic generation imaging

Second-harmonic generation (SHG) imaging of NTG and cMyBP-C$^{\Delta C10mut}$ hearts was performed and quantified as we previously described.[40]

2.6 Cardiac muscle organization analysis

To examine whole heart morphology, hearts from NTG and cMyBP-C$^{\Delta C10mut}$ animals were processed and imaged as described previously.[41]

2.7 Western blot analysis

The level of endogenous cMyBP-C and cMyBP-C$^{\Delta C10mut}$ was evaluated by western blot analysis using both cMyBP-C (polyclonal) and anti-Myc antibody tag (Roche) antibodies in whole heart and myofilament isolations. Following our previously described method, we used a calibration curve of both cMyBP-C and Myc antibodies to perform semi-quantitative analysis.[37] In addition to total protein levels, cMyBP-C phosphorylation was determined by using site-specific phospho-antibodies, as described previously.[21]

2.8 Force-calcium relationship in *permeabilized cardiomyocytes*

Isometric force measurements on permeabilized myocytes were performed, as described before.[42]

2.9 Electron microscopy

Hearts were dissected and then fixed with glutaraldehyde/paraformaldehyde. For sectioning, fixed muscles were post-fixed with 1% OsO_4 in 0.1 M sodium cacodylate buffer for 1 h, dehydrated in graded alcohol and then embedded in Epon. Ultrathin sections were cut with a diamond knife on a Leica UC7 Ultramicrotome. A-band length, M-line width, and Z-line width were measured using ImageJ.[43] The averaged data were analysed for statistical significance in GraphPad Prism using a one-way analysis of variance (ANOVA) with Tukey's multiple comparison test.

2.10 Statistical analyses

Tension-pCa relationships were fit with a modified Hill equation.[44–46] The data are presented as mean ± SEM. Normal distribution of data was tested with the Shapiro–Wilk test. If data were normally distributed, a Student's *t*-test was used to determine significant differences between groups. The Mann–Whitney *U* test was used for non-normal distribution of data. Statistically significant differences were considered as $P < 0.05$.

3. Results

3.1 TG expression of cMyBP-C$^{\Delta C10mut}$ causes HCM in mice

Data gained from previous *in vitro* experiments showed that cMyBP-C$^{\Delta C10mut}$ could not properly incorporate in adult rat cardiomyocytes which resulted in decreased sarcomere contractility.[37] However, it is unknown whether abnormal localization of cMyBP-C$^{\Delta C10mut}$ or its overexpression can cause HCM *in vivo*. A knock-in model of this mutation was considered unsuitable because mouse intron 32 is entirely different from that of human, and ablation of exon 33 would result in a different stop codon when compared with human. Therefore, a cardiac-specific TG mouse model expressing cMyBP-C$^{\Delta C10mut}$ was established (*Figure 1A*) to determine the physiological changes that result from the presence of cMyBP-C$^{\Delta C10mut}$ and to define the functional defects underlying HCM. High levels of transgene expression were seen at the mRNA level (*Figure 1B*, panel left), as primers recognizing both endogenous and TG *Mybpc3* showed 19.6 ± 1.3-fold higher expression in cMyBP-C$^{\Delta C10mut}$ mice than NTG littermates, while primers recognizing only endogenous *Mybpc3* showed a slightly lower expression in cMyBP-C$^{\Delta C10mut}$ compared with NTG (*Figure 1B*, panel right). Analysis at the protein level revealed no significant change in total cMyBP-C levels (*Figure 1C*) or myofilament cMyBP-C levels (Supplementary material online, *Figure S1A–C*). cMyBP-C is heavily regulated by phosphorylation; therefore, the phosphorylation levels of the four most common sites were evaluated, but these were found to be unchanged (Supplementary material online, *Figure S2*). Additionally, cardiac troponin I (cTnI) phosphorylation was unchanged between the groups (Supplementary material online, *Figure S1A, B,* and *D*). Most HCM-associated *MYBPC3* mutations lead to premature stop codons, resulting in mRNA degradation by nonsense-mediated decay (NMD) and/or quick degradation of the truncated protein.[11,47] To establish if this is true for cMyBP-C$^{\Delta C10mut}$, the percentage of cMyBP-C derived from the c-Myc-tagged transgene was determined. In cMyBP-C$^{\Delta C10mut}$ mice, 31.6 ± 6.2% of cMyBP-C was derived from the transgene (i.e. c-Myc tagged, *Figure 1D*). These data show that the cMyBP-C$^{\Delta C10mut}$ protein can be translated and remain stable enough for detection. Thus, any pathological effect elicited by cMyBP-C$^{\Delta C10mut}$ could be attributed to a poison polypeptide effect, or, in the alternative, through dysregulation of RNA or protein degradation pathways. This model is, therefore, suitable for studying the pathophysiological consequences of cMyBP-C$^{\Delta C10mut}$.

3.2 Augmented fibrosis is evident in cMyBP-C$^{\Delta C10mut}$ hearts

We next asked whether cMyBP-C$^{\Delta C10mut}$ expression alone would be sufficient to cause HCM in mice. Indeed, cMyBP-C$^{\Delta C10mut}$ expression resulted in increased heart size and weight compared with NTG mice (*Figure 2A*). A characteristic of HCM is myocardial fibrosis.[48] Thus, histopathological analyses using myocardial sections from cMyBP-C$^{\Delta C10mut}$ and NTG hearts was performed. Percent nuclear area, an indicator of cellularity, was significantly elevated in cMyBP-C$^{\Delta C10mut}$ hearts (*Figure 2B and C*). Similarly, significant fibrosis was noticed in cMyBP-C$^{\Delta C10mut}$ myocardial sections, as shown by increased Masson's trichrome staining (*Figure 2B* and *D*). This was confirmed with SHG imaging (collagen deposition, *Figure 2E* and *G*). SHG was also used to quantify sarcomere area (*Figure 2E* and *F*) and revealed a significant increase in sarcomere area in cMyBP-C$^{\Delta C10mut}$ myocardial sections compared with those from NTG mice. Together, these data demonstrate that myocardial fibrosis

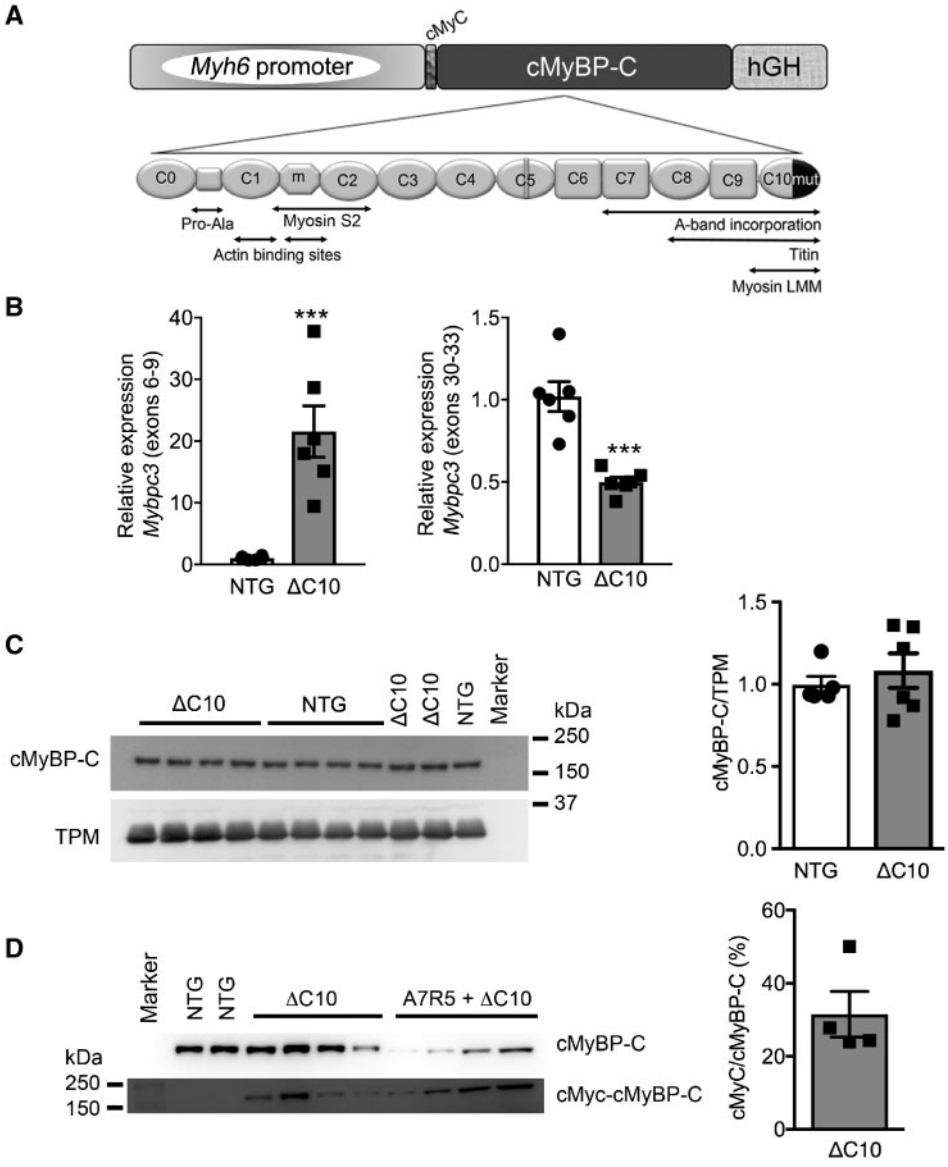

Figure 1 Cardiac-specific TG expression of cMyBP-C$^{\Delta C10mut}$. (*A*) Schematic diagram of the TG construct expressing the cMyBP-C$^{\Delta C10mut}$ (ΔC10) under the control of α-myosin heavy chain promoter. (*B*) mRNA gene expression levels of *MYBPC3* using primers targeting endogenous cMyBP-C and TG cMyBP-C$^{\Delta C10mut}$ (left) or endogenous cMyBP-C only (right) from NTG vs. cMyBP-C$^{\Delta C10mut}$ ($n = 6$). Quantification of cMyBP-C$^{\Delta C10mut}$ expression relative to total cMyBP-C. (*C*) Western blot analysis showing total cMyBP-C expression in NTG and cMyBP-C$^{\Delta C10mut}$ hearts (left) and their quantification normalized to the internal loading control α-tropomyosin (TPM) (5 NTG and 6 ΔC10). (*D*) Western blot analysis depicting total cMyBP-C and the c-Myc-tagged cMyBP-C$^{\Delta C10mut}$ in NTG and cMyBP-C$^{\Delta C10mut}$ mice, as well as adenovirus-expressed cMyBP-C$^{\Delta C10mut}$ in A7R5 rat aortic smooth muscle cells (left) ($n = 4$ ΔC10). ***$P < 0.001$.

accompanies cardiac remodelling in cMyBP-C$^{\Delta C10mut}$ mice, further implicating that cMyBP-C$^{\Delta C10mut}$ expression leads to the macroscopic changes seen in HCM.

3.3 cMyBP-C$^{\Delta C10mut}$ mice show cardiac hypertrophy and diastolic dysfunction

cMyBP-C$^{\Delta C10mut}$ protein expression caused hypertrophy in 3-month-old animals (*Figures 2* and *3A*). In line with this finding, morphometric measurements revealed a significant elevation in LV wall diameter and area (*Figure 3B and C*), right ventricular wall diameter and volume (*Figure 3D* and *E*), and heart width (*Figure 3G*) in cMyBP-C$^{\Delta C10mut}$ hearts compared with NTG controls. No significant difference in heart height was observed between cMyBP-C$^{\Delta C10mut}$ and NTG mice (*Figure 3F*). To evaluate cardiac function in cMyBP-C$^{\Delta C10mut}$ hearts compared with NTG controls, short-axis M-mode echocardiography was performed (*Figure 4A*). In keeping with an early HCM phenotype, systolic function was elevated (*Figure 4B* and *C*), while diastolic function, as determined by blood and tissue Doppler measurements, was impaired (*Figure 4D*) in cMyBP-C$^{\Delta C10mut}$ hearts compared with NTG controls. Evaluation of percent global longitudinal strain (GLS) in cMyBP-C$^{\Delta C10mut}$ hearts compared with NTG controls revealed no difference (*Figure 4E*). No other

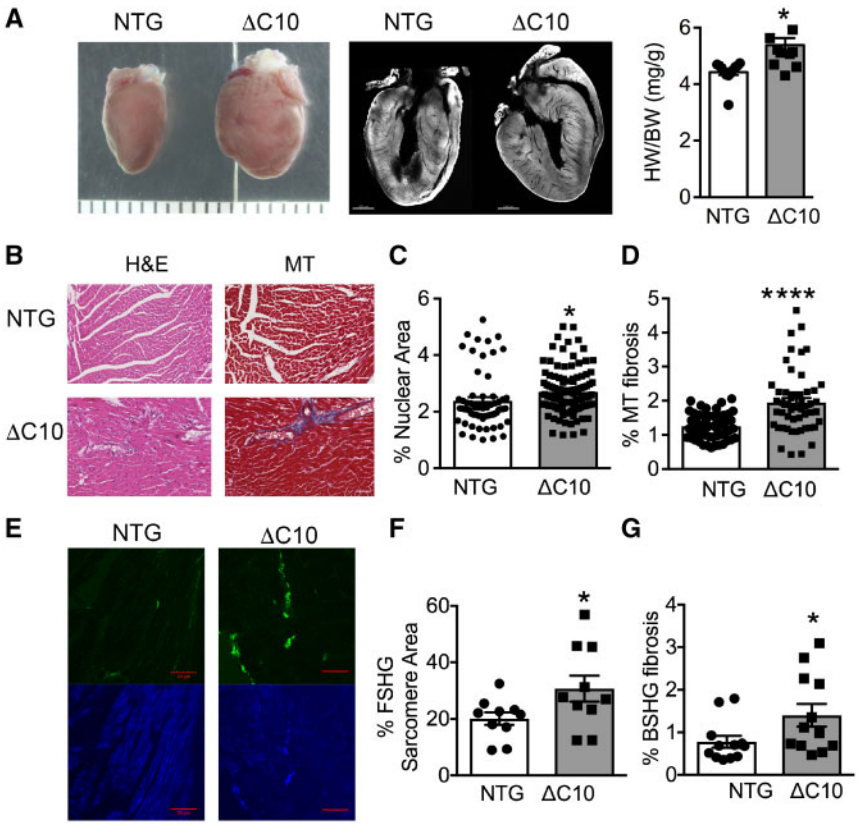

Figure 2 Myocardial fibrosis is elevated in cMyBP-C$^{\Delta C10mut}$ hearts. (*A*) Gross morphology, cross section of whole isolated hearts and heart/body weight (HW/BW) ratio (mg/g). Scale marks are separated by 1000 µm in left panel and scale bar = 1000 µm in middle panel. (*B*) Representative H&E- and Masson trichrome (MT)-stained myocardial sections from cMyBP-C$^{\Delta C10mut}$ and NTG hearts. Scale bar = 50 µm. (*C*) Quantification of percent nuclear area and (*D*) percent MT fibrosis obtained from measurements of H&E- and MT-labelled myocardial sections from cMyBP-C$^{\Delta C10mut}$ and NTG hearts (n = 3 NTG hearts, 62 sections and 3 cMyBP-C$^{\Delta C10mut}$ hearts, 106 sections for panel C and n = 3 NTG hearts, 53 sections and 3 cMyBP-C$^{\Delta C10mut}$ hearts, 52 sections for *D*). (*E*) Representative SHG-imaged myocardial sections from cMyBP-C$^{\Delta C10mut}$ and NTG hearts. The green channel is backward SHG (BSHG) predominantly depicting collagen fibres, and the blue channel is forward-directed SHG (FSHG) showing the sarcomere pattern. Scale bar = 20 µm. Quantification of (*F*) percent FSHG sarcomere area and (*G*) percent BSHG fibrosis obtained from SHG-imaged myocardial sections from cMyBP-C$^{\Delta C10mut}$ and NTG hearts (n = 3 NTG hearts, 10 sections and 3 cMyBP-C$^{\Delta C10mut}$ hearts, 10 sections for *F* and n = 3 NTG hearts, 12 sections and 3 cMyBP-C$^{\Delta C10mut}$ hearts, 13 sections for *G*). *P < 0.05, ****P < 0.0001.

significant changes in cardiac function or morphology were seen by echocardiography (*Table 1*). cMyBP-C$^{\Delta C10mut}$ expression caused diastolic, but not systolic dysfunction, a pattern that is typical of HCM. Together, these data indicate that expression of cMyBP-C$^{\Delta C10mut}$ is sufficient to cause cardiac hypertrophy.

3.4 cMyBP-C$^{\Delta C10mut}$ myofilaments exhibit increased Ca^{2+}-sensitivity

We next evaluated whether the diastolic dysfunction that was observed through echocardiography (*Figure 4D*) also occurred at the myofilament level. Maximal force-generating capacity of permeabilized cardiomyocytes did not change between cMyBP-C$^{\Delta C10mut}$ and NTG mice (*Figure 5A* and *C*), while an increased Ca^{2+}-sensitivity of force development was observed in cMyBP-C$^{\Delta C10mut}$ cardiomyocytes (*Figure 5B* and *D*). When cardiomyocyte ultrastructure was studied by electron microscopy, no changes were apparent in thick filament length or arrangement, or in M-line or Z-line structure and dimensions (Supplementary material online, *Figure S3*). *In vivo* and *in vitro* contractile analyses indicated altered relaxation in cMyBP-C$^{\Delta C10mut}$ hearts owing to changes in myofilament Ca^{2+}-sensitivity.

3.5 Gene pathway enrichment analyses and network visualization

To determine the global gene expression changes in cMyBP-C$^{\Delta C10mut}$ hearts compared with NTG controls, we performed RNA-seq analysis using total mRNA isolated from the hearts of these mice (*Figure 6*). In total, we observed 222 upregulated and 299 downregulated genes in cMyBP-C$^{\Delta C10mut}$ compared with NTG hearts. As expected, total *Mybpc3* gene expression was highly up-regulated in cMyBP-C$^{\Delta C10mut}$ compared with NTG hearts by the TG overexpression of cMyBP-C$^{\Delta C10mut}$. Supporting the observed increased heart size and wall thickness, we detected an upregulation of several hypertrophy genes, including *Myh7* and *Nppa*, in cMyBP-C$^{\Delta C10mut}$ hearts. We next performed gene ontology analyses of this RNA-Seq dataset for biological processes

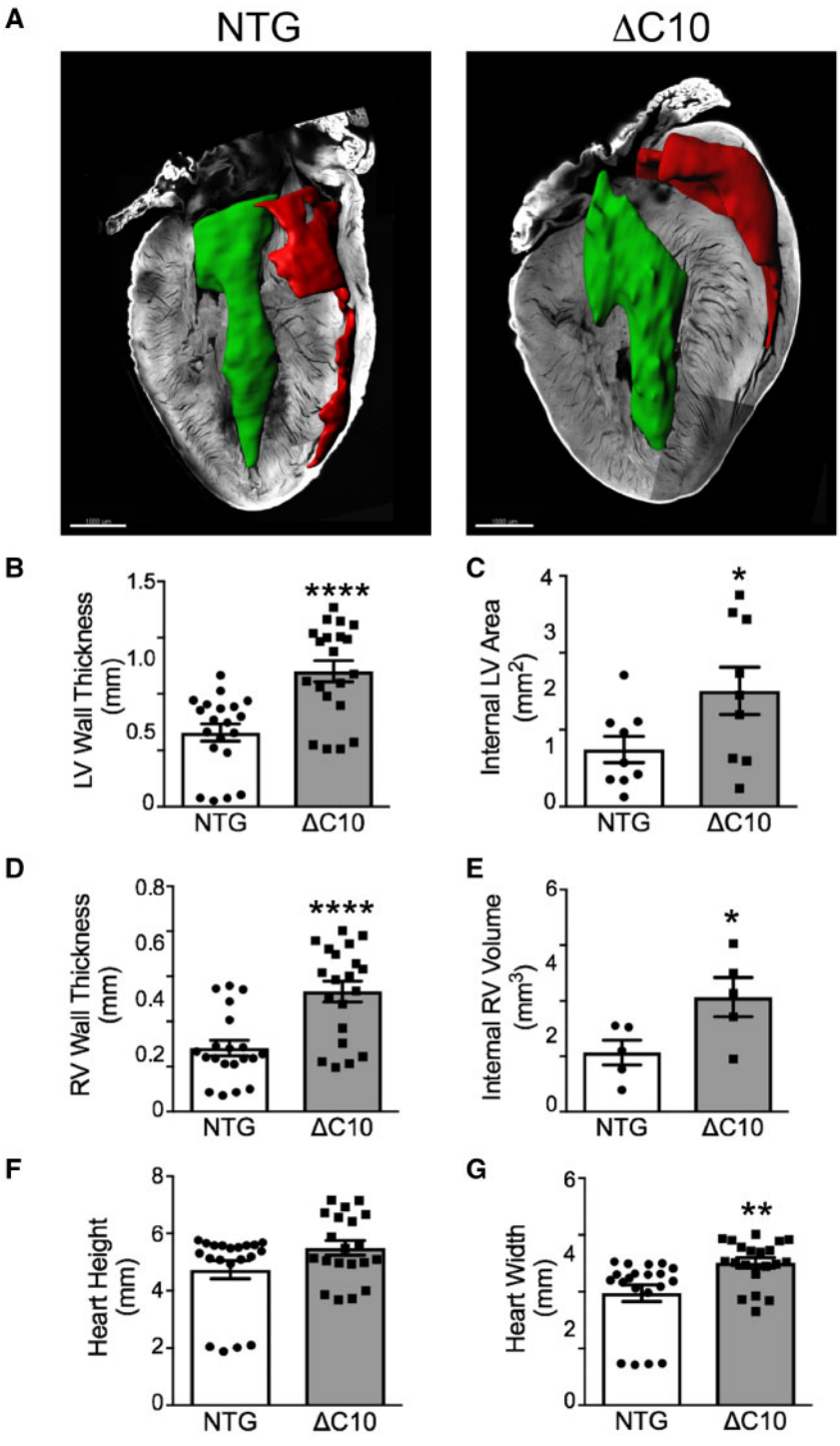

Figure 3 cMyBP-C$^{\Delta C10mut}$ hearts display myocardial hypertrophy. (*A*) Confocal microscopy of myocardial sections from NTG and cMyBP-C$^{\Delta C10mut}$ hearts with cardiac chambers artificially filled with blood. Scale bar = 1000 μm. Morphometric measurements of confocal myocardial sections from NTG and cMyBP-C$^{\Delta C10mut}$ hearts quantifying (*B*) LV wall thickness, (*C*) Internal LV area, (*D*) RV wall thickness, (*E*) internal RV volume, (*F*) heart height, and (*G*) heart width (n = 5 NTG, 5 ΔC10). *P < 0.05, **P < 0.01, ****P < 0.0001.

and pathways that were overrepresented or underrepresented in cMyBP-C$^{\Delta C10mut}$ compared with NTG hearts, as we described previously.[49] Selected enriched biological processes and pathways in cMyBP-C$^{\Delta C10mut}$ compared with NTG hearts are depicted in the network representation in *Figure 6B*.

3.6 cMyBP-C$^{\Delta C10mut}$ protein mislocalizes at the Z-line

It has been established that the cMyBP-C$^{\Delta C10mut}$ leads to the replacement of 62 of the C-terminal amino acids with a non-native sequence of

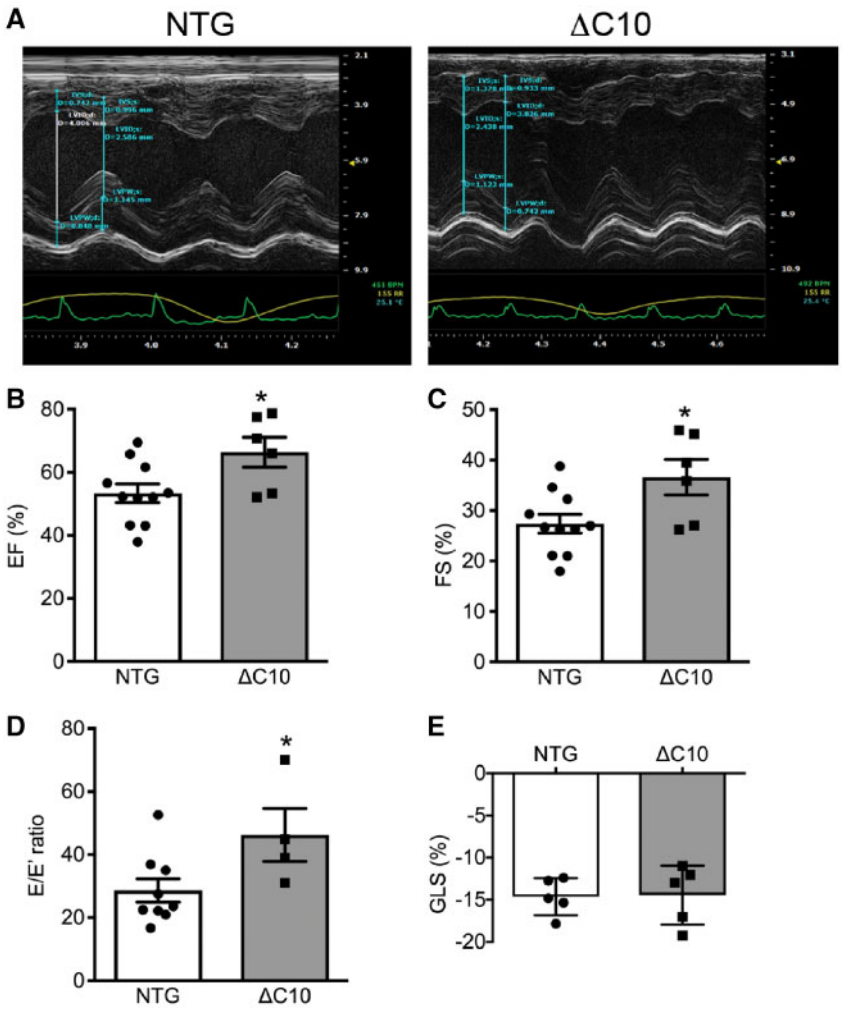

Figure 4 Diastolic dysfunction in cMyBP-C$^{\Delta C10mut}$ mice. (*A*) M-mode echocardiographic tracings showing LV hypertrophy in cMyBP-C$^{\Delta C10mut}$ hearts. Echocardiographic analysis of (*B*) ejection fraction (EF, %), (*C*) fractional shortening (FS, %), (*D*) *E*/*E*′ ratio and (*E*) global longitudinal strain analysis (GLS, %) ($n = 6$) *$P < 0.05$.

Table 1 Echocardiographic data and cardiomyocyte force-Ca^{2+} data of NTG and cMyBP-C$^{\Delta C10mut}$ TG mice

	NTG	cMyBP-C$^{\Delta C10mut}$	*P*-value	*n* value (NTG vs. cMyBP-C$^{\Delta C10mut}$)
HW/BW (mg/g)	4.43 ± 0.11	5.38 ± 0.24	0.02*	12 vs. 11
IVSTd (mm)	0.77 ± 0.05	0.82 ± 0.04	0.53	11 vs. 7
IVSTs (mm)	1.18 ± 0.05	1.23 ± 0.08	0.54	11 vs. 7
LVPWd (mm)	0.80 ± 0.05	0.77 ± 0.02	0.98	11 vs. 7
LVPWs (mm)	1.06 ± 0.08	1.14 ± 0.07	0.47	11 vs. 7
LVIDd (mm)	3.98 ± 0.17	3.61 ± 0.17	0.16	11 vs. 7
LVIDs (mm)	2.90 ± 0.16	2.39 ± 0.18	0.05	11 vs. 7
EF (%)	53.4 ± 2.9	66.4 ± 4.7	0.03*	11 vs. 7
FS (%)	27.4 ± 1.9	36.6 ± 3.5	0.02*	11 vs. 7
GLS (%)	-13.0 ± -1.0	-13 ± -1.1	0.98	5 vs. 5
E/*A*	1.66 ± 0.09	1.64 ± 0.10	0.88	6 vs. 6
E/*E*′	28.7 ± 3.7	46.3 ± 8.4	0.04*	6 vs. 6
F_{max} (kN/m^2)	19.96 ± 2.2	24.62 ± 3.4	0.36	5 vs. 10
EC^{50} (μM)	3.58 ± 0.33	2.74 ± 0.13	0.018*	5 vs. 10

Summary of the heart weight (HW) to body weight (BW) ratio, echocardiographic findings, and functional measurements of cardiomyocytes from cMyBP-C$^{\Delta C10mut}$ compared with NTG hearts. *P*-values were calculated by two-tailed unpaired Student's *t*-tests.
*$P < 0.05$.

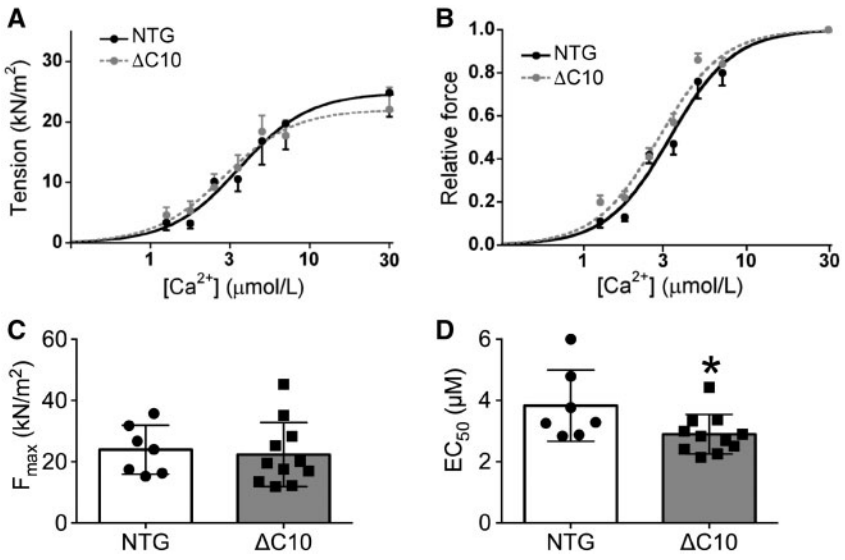

Figure 5 Increased myofilament Ca^{2+}-sensitivity of force generation in cMyBP-$C^{\Delta C10mut}$ skinned myocytes. Functional measurements of cardiomyocytes isolated from NTG and cMyBP-$C^{\Delta C10mut}$ hearts showing (*A*) force-Ca^{2+}, (*B*) relative force curves, (*C*) maximal force, and (*D*) EC_{50} values ($n = 5$ NTG, 10 cMyBP-$C^{\Delta C10mut}$). $^*P < 0.042$.

55 residues. This includes the four out five of critical amino acids crucial for binding to the rod domain of myosin heavy chain.[21] We and others have shown that this domain is crucial for incorporation into the sarcomere; therefore, the amount of cMyBP-C in the soluble fraction (i.e. non-sarcomere) was studied. Levels of cMyBP-C in the soluble fraction were increased 22.5 ± 6.8-fold in cMyBP-$C^{\Delta C10mut}$ mice vs. NTG controls (*Figure 7A*). The apparent mislocalization of cMyBP-C was confirmed with immunofluorescence staining of isolated cardiomyocytes from cMyBP-$C^{\Delta C10mut}$ and NTG hearts (*Figure 7B* and *C*). Staining with an antibody raised against the N-terminus of cMyBP-C resulted in the typical doublet staining between each actinin-labelled Z-line (*Figure 7B*). In contrast, localization of cMyBP-$C^{\Delta C10mut}$, as specifically identified with an antibody raised against the c-Myc tag, was not restricted to the C-zone of the sarcomere, but was, instead, present at the Z-line with some diffuse, randomly distributed staining along the rest of the sarcomere (*Figure 7C*). This suggests that mislocalization of cMyBP-$C^{\Delta C10mut}$ at the Z-line in cMyBP-$C^{\Delta C10mut}$ cardiomyocytes could cause the contractile abnormalities, as observed in the hearts of these animals, and trigger myocardial remodelling leading to HCM.

4. Discussion

The cMyBP-$C^{\Delta C10mut}$ variant is associated with the development of various forms of cardiomyopathy and HF, but its functional and molecular effects are unknown.[19] Seventy percent of all *MYBPC3* mutations, including cMyBP-$C^{\Delta C10mut}$, are predicted to produce proteins that have premature stops or frame shifts that terminate or change the C'-terminal, which includes key myosin-binding residues. These truncated protein products are either not expressed or quickly degraded, as expression of the mutant protein cannot be found in cardiac tissue from HCM patients.[23,28,50] This means that reduced cMyBP-C expression, i.e. haploinsufficiency, rather than detrimental effects of the mutant protein, i.e. poison polypeptide, is the predominant disease mechanism of *MYBPC3* truncation mutants,[51,52] but the aetiology of HCM in heterozygous *MYBPC3* truncation mutation carriers may vary depending on the specific mutation.

The genotype–phenotype relationship in HCM is far from straightforward. The same mutation can lead to HCM development at young age in one person, while a family member could live symptom-free until late age. This was illustrated in a recent study in which genotype–positive/phenotype–negative subjects (family members of overt HCM patients) were monitored for almost two decades.[38] The study determined that carrying the cMyBP-$C^{\Delta C10mut}$ does not mean that disease will develop, at least not at a young age.[38] It is possible that some mutations are more penetrant than others, but this needs to be established. Studying the disease mechanisms of specific *MYBPC3* mutations is complicated by the occurrence of mutations in other sarcomeric proteins, resulting in worse prognoses.[34] For example, if carriers of cMyBP-$C^{\Delta C10mut}$ also carry a mutation in *MYH7*, this combination frequently results in sudden cardiac death.[33] More shocking statistics indicate that South Asians carrying the cMyBP-$C^{\Delta C10mut}$ have 50% higher rates of morbidity and mortality after ischaemia–reperfusion injury compared with other ethnic groups.[53–55] Supporting these data, Srivastava *et al.*[36] showed that the presence of cMyBP-$C^{\Delta C10mut}$ leads to reduced contractile function following coronary artery disease, suggesting that cMyBP-$C^{\Delta C10mut}$ pathogenicity can exacerbate cardiac dysfunction in patients with myocardial infarction.

To the best of our knowledge, the pathological consequences of cMyBP-$C^{\Delta C10mut}$ expression have never been studied *in vivo*. Given its presence in and potential impact on 100 million people of South Asian descent worldwide, systematically studying the presumed expression of cMyBP-$C^{\Delta C10mut}$ at the whole-organ level would have clear translational value. The cMyBP-$C^{\Delta C10mut}$ mutation was initially described in a group of Indian HCM patients in 2003.[34] In a more extensive follow-up study using a large cohort of cardiomyopathy cases and healthy controls, this mutation was shown to be a founder mutation highly prevalent among South Asians (6%).[38] The mutation was overrepresented in the

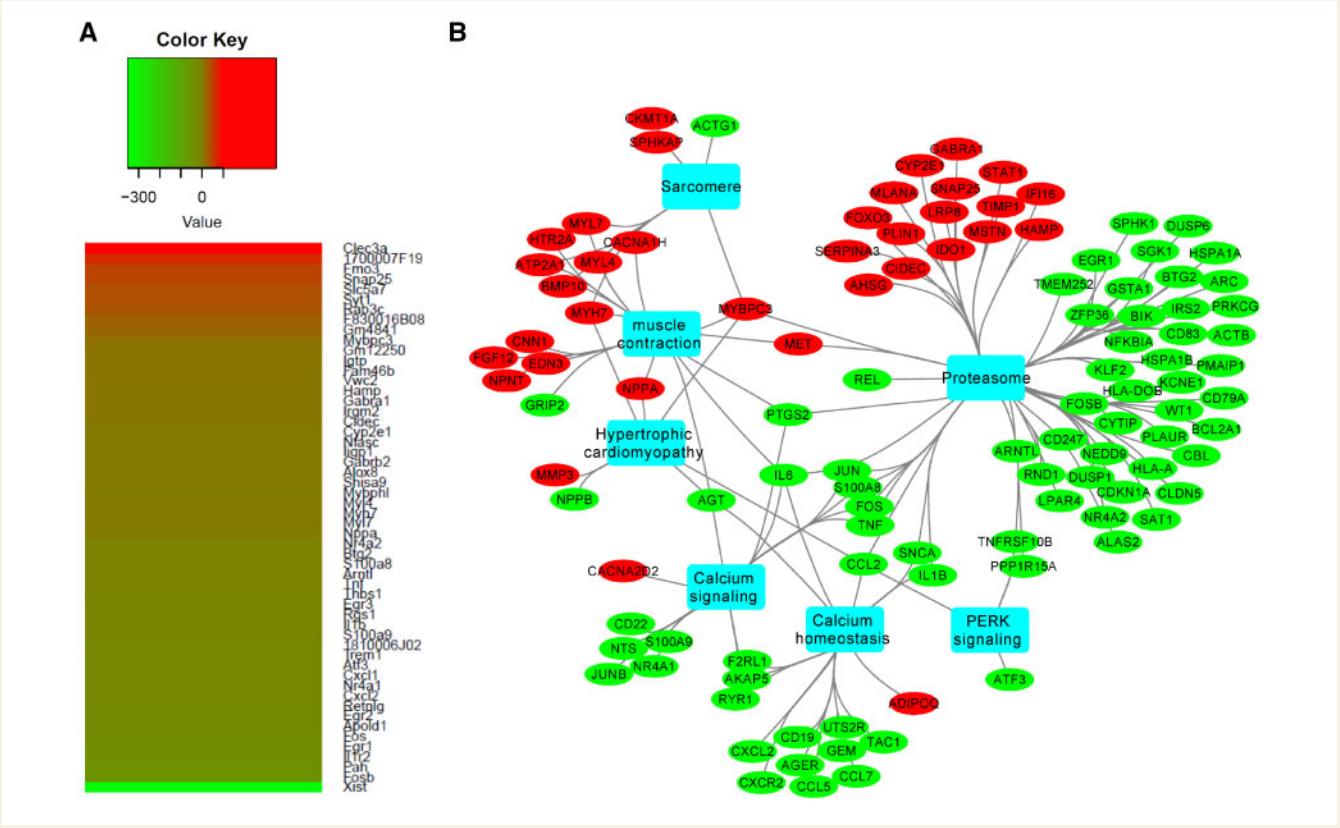

Figure 6 Differentially regulated genes in cMyBP-C$^{\Delta C10mut}$ compared with NTG hearts. (*A*) RNA-seq heat maps depicting clusters of genes differentially regulated in cMyBP-C$^{\Delta C10mut}$ vs. NTG hearts. Shown is a subset of the most up-regulated (red) and down-regulated (green) genes from the total gene set. The fold change, up or down, is represented in the key for the respective panels ($n = 4$ pooled samples per genotype). (*B*) Network of significantly enriched gene ontology terms for upregulated genes in cMyBP-C$^{\Delta C10mut}$ hearts. The red and green circles denote upregulated and downregulated genes, respectively, in cMyBP-C$^{\Delta C10mut}$ compared with NTG hearts. Blue rectangles represent significantly enriched ($P < 0.05$; FDR) biological processes using the ToppFun application of ToppGene Suite.

cardiomyopathy group, indicating that carrying the mutation confers a greater risk of developing cardiomyopathy. Of note, carrying the mutation could lead to HCM, but it could also lead to dilated cardiomyopathy to a similar degree, or to restrictive cardiomyopathy to a lesser degree.[19] In a recent study, we found a similarly high mutation frequency in people of South Asian descent living in the USA (6.0%).[38] The screening performed in this study was done on people attending community events, not a hospital setting. Therefore, most people were free of cardiac disease. In this group of subjects, we did not find an increase in systolic or diastolic dysfunction measured by echocardiography. This discrepancy could be explained if cMyBP-C$^{\Delta C10mut}$ causes late disease onset. Most people screened (84.5%) were under the age of 60.[38] Founder mutations can subsist in the population if they are associated with a mild phenotype or a late disease onset.

We performed cardiomyopathy panel screening on this cohort and identified a second, previously undescribed, mutation on the same *MYBPC3* allele, D389V. This mutation strongly correlated with hyperdynamic ventricular function and ventricular wall thickening.[38] The D389V mutation sits at a critical regulatory region of cMyBP-C that may alter the ability of cMyBP-C to regulate actomyosin interactions, but future studies are needed to directly assess the function of this mutation. Because this missense mutation was strongly linked to HCM and occurred on the same allele as that of the cMyBP-C$^{\Delta C10mut}$, it can be argued that this mutant protein must at least be translated to exert a pathophysiological function, whether by improper binding and resultant myofilament dysregulation, or by a protein aggregation mechanism. This information provides support for studying the TG expression of cMyBP-C$^{\Delta C10mut}$ in mice at the whole-heart level.

By examining its underlying molecular mechanism, the present study aimed to determine the sufficiency of cMyBP-C$^{\Delta C10mut}$ expression as a causative factor in the development of an HCM phenotype. We have demonstrated that TG expression of cMyBP-C$^{\Delta C10mut}$ in mouse hearts *in vivo* results in a phenotype of HCM with hypertrophy, diastolic dysfunction, and fibrosis. Indeed, this was supported by earlier *in vitro* findings showing that expression of cMyBP-C$^{\Delta C10mut}$ in adult rat cardiomyocytes leads to contractile dysfunction.[37] Further *in vitro* analysis showed that the mutant C10 domain loses its ability to interact with the light meromyosin region of myosin heavy chain. The decreased thick filament affinity of the C'-terminal of cMyBP-C$^{\Delta C10mut}$ also explains the increased presence of cMyBP-C in the soluble fraction of cMyBP-C$^{\Delta C10mut}$ heart lysates. Since TG expression of wild-type cMyBP-C in mice did not result in a phenotype,[56,57] we have evidence that the culprit is cMyBP-C$^{\Delta C10mut}$, not high expression levels of cMyBP-C.

The apparent discrepancy between the high levels of non-symptomatic human mutation carriers and the TG mouse data presented in this manuscript, as well as the rat cardiomyocyte data published

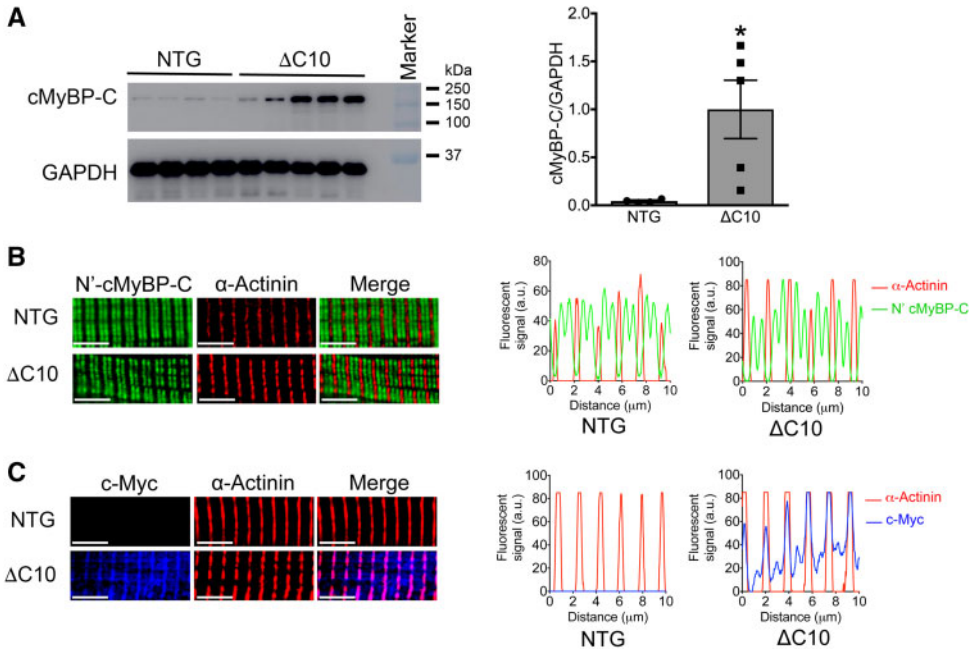

Figure 7 cMyBP-C$^{\Delta C10mut}$ protein is highly soluble and localizes at the Z-line in the cardiac sarcomere. (*A*) Western blot analysis depicting the levels of total soluble cMyBP-C (endogenous and/or cMyBP-C$^{\Delta C10mut}$) from cMyBP-C$^{\Delta C10mut}$ and NTG hearts ($n = 4$ NTG, 5 cMyBP-C$^{\Delta C10mut}$ $*P < 0.027$). (*B*) Single cardiomyocytes were isolated from cMyBP-C$^{\Delta C10mut}$ and NTG hearts and were stained with antibodies detecting cMyBP-C's N-terminus (C0 domain) (green) and α-actinin (red). In both NTG and cMyBP-C$^{\Delta C10mut}$ myocytes, the classical staining pattern of two cMyBP-C bands between Z-lines (stained with α-actinin) was observed, indicating proper localization of endogenous cMyBP-C in cMyBP-C$^{\Delta C10mut}$ and NTG cardiomyoctyes. (*C*) Cardiomyocytes from cMyBP-C$^{\Delta C10mut}$ and NTG hearts were stained with antibodies to detect c-Myc (blue), which will show only the c-Myc-tagged cMyBP-C$^{\Delta C10mut}$ protein and α-actinin (red). The c-Myc signal was only observed in myocytes from cMyBP-C$^{\Delta C10mut}$ hearts. The presence of c-Myc staining at the Z-line with α-actinin suggests that the cMyBP-C$^{\Delta C10mut}$ protein aberrantly distributes within the cardiac sarcomere in cMyBP-C$^{\Delta C10mut}$ myocytes. Scale bar = 5 μm in *B* and *C*.

earlier,[37] could be explained if high expression levels of cMyBP-C$^{\Delta C10mut}$ are needed to induce disease. In both the TG mice and adenoviral-based experiments in rat cardiomyocytes, high expression levels of cMyBP-C$^{\Delta C10mut}$ were induced. At present, the protein level of cMyBP-C$^{\Delta C10mut}$ in human heart tissue is unknown, but it could be that heterozygous cMyBP-C$^{\Delta C10mut}$ carriers express the mutant protein at a low level. If that is the case, the addition of a secondary stressor, whether by a co-mutation or other external factors, could be the trigger leading to cardiomyopathy. It has been shown that carrying cMyBP-C$^{\Delta C10mut}$ leads to greater cardiac dysfunction in post-myocardial infarction patients,[53–55] supporting its role as a disease modifier.

The exact mechanism by which cMyBP-C$^{\Delta C10mut}$ expression leads to dysfunction is unknown. cMyBP-C$^{\Delta C10mut}$ did not localize to its usual position in the C-zone. At least part of the protein localized to the Z-line (*Figure 7*), and upon subcellular fractionation with high levels of detergent we observed increased levels of soluble cMyBP-C$^{\Delta C10mut}$. While the fold change in soluble cMyBP-C between cMyBP-C$^{\Delta C10mut}$ and NTG is sizeable (22.5 fold), it should be noted that the level of soluble cMyBP-C in NTG is very low. So even in the cMyBP-C$^{\Delta C10mut}$, the vast majority of cMyBP-C is likely to be myofilament associated. Our *in vitro* analysis also revealed Z-line staining.[37] It is unknown if this mislocalization contributes to impaired relaxation. As we did not observe an increase of total cMyBP-C in the myofilament fraction (Supplementary material online, *Figure S1*), despite the Z-disc staining of cMyBP-C$^{\Delta C10mut}$, it could be possible that endogenous cMyBP-C expression is lower. We did indeed observe a lower mRNA expression of endogenous cMyBP-C (*Figure 1B*, right panel). A lower level of cMyBP-C and cMyBP-C$^{\Delta C10mut}$ that localizes to the Z-line rather than C-zone could cause C-zone haploinsufficiency. From studies in mouse models and HCM patients, we know that haploinsufficiency of cMyBP-C could lead to increased calcium sensitivity.[58–60] We did observe an increased calcium sensitivity of force development that was not caused by decreased cTnI phosphorylation. In a mouse model of a truncating cMyBP-C mutation, a bigger shift in calcium sensitivity was seen,[58] but in another study using the same mouse model an increase of a similar magnitude as the present study was observed.[59] This same shift is also seen in myectomy tissue from HCM patients with a *MYBPC3* mutation.[60] However, the mechanism by which cMyBP-C$^{\Delta C10mut}$ leads to increased calcium sensitivity is unknown. Recent studies have revealed another possible pathogenic effect of cMyBP-C haploinsufficiency: a reduction in the level of myosin that is in the super-relaxed state. The super-relaxed state of myosin is a low energy consuming state and is dependent on cMyBP-C.[61] In HCM patients with a *MYBPC3* mutation leading to haploinsufficiency, reduced levels of super-relaxed myosin were observed.[62] This could lead to increased energy consumption that could contribute to HCM pathophysiology. Indeed, treatment of mouse cardiomyocytes with reduced cMyBP-C levels with a compound that restored the levels of super-relaxed myosin normalized contractile performance.[63] Whether changes in the super-relaxed state are present and contribute to pathology in the cMyBP-C$^{\Delta C10mut}$ model remains to be studied.

Generally, truncating mutations in *MYBPC3* appear to act via haploinsufficiency, although additional lines of inquiry have looked into the possibility that these truncated mutants can dysregulate the NMD or proteasomal pathways as a primary or secondary disease mechanism.[6] While a clear relationship between *MYBPC3* mutations and these degradation pathways has not emerged, data do suggest that altering the ubiquitin-proteasome system can alter disease progression.[6] In our RNA-seq analysis, many genes associated with proteasome function were differentially expressed. Since the proteasome is involved in the degradation of proteins and is known to be involved in HCM pathophysiology,[10,64] it is not surprising to find that it is differentially regulated in the cMyBP-C$^{\Delta C10mut}$ group. Whether or not the high expression of mutant protein overwhelms the proteasome system and whether activation of the system would be a therapeutic strategy[6] requires further study.

In conclusion, we showed that TG expression of cMyBP-C$^{\Delta C10mut}$ leads to all the hallmarks of HCM in mice. However, recent data from people carrying the cMyBP-C$^{\Delta C10mut}$ mutation imply that a heterozygous cMyBP-C$^{\Delta C10mut}$ mutation causes late-onset HCM[17–19] or functions as a disease modifier in HCM[17–19] or may not be pathogenic under baseline normal conditions.[38] Follow-up studies should focus on elucidating the effects of carrying heterozygous cMyBP-C$^{\Delta C10mut}$ mutation in humans and whether the 25-base pair deletion results in exon 33 skipping. If so, we should investigate the underlying mechanism and the likelihood of skipping, as these data could have clinical implications for the large group of mutation carriers living in the USA or abroad.

Supplementary material

Supplementary material is available at *Cardiovascular Research* online.

Acknowledgements

We acknowledge Suresh Govindan, PhD, for his help in cloning cMyBP-C$^{\Delta C10mut}$, mouse genotyping, breeding, and colony management.

Conflict of interest: S.S. provided consulting and collaborative services to AstraZeneca, Merck, and Amgen unrelated to the content of this manuscript. All other authors declared no conflict of interest.

Funding

S.S. has received support from National Institutes of Health grants R01 HL130356, R56 HL139680, R01 AR067279, and R01 HL105826; American Heart Association Cardiovascular Genome-Phenome Study (15CVGPSD27020012) and Catalyst (17CCRG33671128) awards; and AstraZeneca, Merck and Amgen. D.Y.B. (11PRE7240022), D.W.D.K. (13POST17220009), and T.L.L. (15PRE22430028) were supported with American Heart Association fellowship training grants. R.C. was supported by NIH grants P01 HL059408 and R01 HL139883. R.N.-S. has received support from NHLBI grants 1RHL118067 and 2RHL118067.

References

1. Semsarian C, Ingles J, Maron MS, Maron BJ. New perspectives on the prevalence of hypertrophic cardiomyopathy. *J Am Coll Cardiol* 2015;**65**:1249–1254.
2. Authors/Task Force members, Elliott PM, Anastasakis A, Borger MA, Borggrefe M, Cecchi F, Charron P, Hagege AA, Lafont A, Limongelli G, Mahrholdt H, McKenna WJ, Mogensen J, Nihoyannopoulos P, Nistri S, Pieper PG, Pieske B, Rapezzi C, Rutten FH, Tillmanns C, Watkins H. 2014 ESC Guidelines on diagnosis and management of hypertrophic cardiomyopathy: the task force for the diagnosis and management of hypertrophic cardiomyopathy. *Russ J Cardiol* 2014;**35**:2733–2779.
3. Richard P, Charron P, Carrier L, Ledeuil C, Cheav T, Pichereau C, Benaiche A, Isnard R, Dubourg O, Burban M, Gueffet JP, Millaire A, Desnos M, Schwartz K, Hainque B, Komajda M. Hypertrophic cardiomyopathy: distribution of disease genes, spectrum of mutations, and implications for a molecular diagnosis strategy. *Circulation* 2003;**107**:2227–2232.
4. Gupta MK, Gulick J, Liu R, Wang X, Molkentin JD, Robbins J. Sumo E2 enzyme UBC9 is required for efficient protein quality control in cardiomyocytes. *Circ Res* 2014;**115**:721–729.
5. Wang X, Robbins J. Proteasomal and lysosomal protein degradation and heart disease. *J Mol Cell Cardiol* 2014;**71**:16–24.
6. Schlossarek S, Singh SR, Geertz B, Schulz H, Reischmann S, Hubner N, Carrier L. Proteasome inhibition slightly improves cardiac function in mice with hypertrophic cardiomyopathy. *Front Physiol* 2014;**5**:484.
7. Bahrudin U, Morikawa K, Takeuchi A, Kurata Y, Miake J, Mizuta E, Adachi K, Higaki K, Yamamoto Y, Shirayoshi Y, Yoshida A, Kato M, Yamamoto K, Nanba E, Morisaki H, Morisaki T, Matsuoka S, Ninomiya H, Hisatome I. Impairment of ubiquitin-proteasome system by E334K cMyBPC modifies channel proteins, leading to electrophysiological dysfunction. *J Mol Biol* 2011;**413**:857–878.
8. Sandri M, Robbins J. Proteotoxicity: an underappreciated pathology in cardiac disease. *J Mol Cell Cardiol* 2014;**71**:3–10.
9. Wang W, Li S, Wang H, Li B, Shao L, Lai Y, Horvath G, Wang Q, Yamamoto M, Janicki JS, Wang XL, Tang D, Cui T. Nrf2 enhances myocardial clearance of toxic ubiquitinated proteins. *J Mol Cell Cardiol* 2014;**72**:305–315.
10. Dorsch LM, Schuldt M, Knezevic D, Wiersma M, Kuster DWD, van der Velden J, Brundel B. Untying the knot: protein quality control in inherited cardiomyopathies. *Pflugers Arch* 2019;**471**:795–806.
11. Vignier N, Schlossarek S, Fraysse B, Mearini G, Kramer E, Pointu H, Mougenot N, Guiard J, Reimer R, Hohenberg H, Schwartz K, Vernet M, Eschenhagen T, Carrier L. Nonsense-mediated mRNA decay and ubiquitin-proteasome system regulate cardiac myosin-binding protein C mutant levels in cardiomyopathic mice. *Circ Res* 2009;**105**:239–248.
12. Carrier L. Too much of a good thing is bad: proteasome inhibition induces stressed hearts to fail. *Cardiovasc Res* 2010;**88**:389–390.
13. Carrier L, Schlossarek S, Willis MS, Eschenhagen T. The ubiquitin-proteasome system and nonsense-mediated mRNA decay in hypertrophic cardiomyopathy. *Cardiovasc Res* 2010;**85**:330–338.
14. Watkins H, Conner D, Thierfelder L, Jarcho JA, MacRae C, McKenna WJ, Maron BJ, Seidman JG, Seidman CE. Mutations in the cardiac myosin binding protein-C gene on chromosome 11 cause familial hypertrophic cardiomyopathy. *Nat Genet* 1995;**11**:434–437.
15. Bonne G, Carrier L, Bercovici J, Cruaud C, Richard P, Hainque B, Gautel M, Labeit S, James M, Beckmann J, Weissenbach J, Vosberg H-P, Fiszman M, Komajda M, Schwartz K. Cardiac myosin binding protein-C gene splice acceptor site mutation is associated with familial hypertrophic cardiomyopathy. *Nat Genet* 1995;**11**:438–440.
16. Carrier L, Mearini G, Stathopoulou K, Cuello F. Cardiac myosin-binding protein C (MYBPC3) in cardiac pathophysiology. *Gene* 2015;**573**:188–197.
17. Adalsteinsdottir B, Teekakirikul P, Maron BJ, Burke MA, Gudbjartsson DF, Holm H, Stefansson K, DePalma SR, Mazaika E, McDonough B, Danielsen R, Seidman JG, Seidman CE, Gunnarsson GT. Nationwide study on hypertrophic cardiomyopathy in Iceland: evidence of a MYBPC3 founder mutation. *Circulation* 2014;**130**:1158–1167.
18. Alders M, Jongbloed R, Deelen W, van den WA, Doevendans P, Ten CF, Regitz ZV, Vosberg HP, van LI, Wilde A, Dooijes D, Mannens M. The 2373insG mutation in the MYBPC3 gene is a founder mutation, which accounts for nearly one-fourth of the HCM cases in the Netherlands. *Eur Heart J* 2003;**24**:1848–1853.
19. Dhandapany PS, Sadayappan S, Xue Y, Powell GT, Rani DS, Nallari P, Rai TS, Khullar M, Soares P, Bahl A, Tharkan JM, Vaideeswar P, Rathinavel A, Narasimhan C, Ayapati DR, Ayub Q, Mehdi SQ, Oppenheimer S, Richards MB, Price AL, Patterson N, Reich D, Singh L, Tyler-Smith C, Thangaraj K. A common MYBPC3 (cardiac myosin binding protein-C) variant associated with cardiomyopathies in South Asia. *Nat Genet* 2009;**41**:187–191.
20. Shaffer JF, Kensler RW, Harris SP. The myosin-binding protein C motif binds to F-actin in a phosphorylation-sensitive manner. *J Biol Chem* 2009;**284**:12318–12327.
21. Kuster DW, Sadayappan S. MYBPC3's alternate ending: consequences and therapeutic implications of a highly prevalent 25 bp deletion mutation. *Pflugers Arch* 2014;**466**:207–213.
22. Barefield D, Sadayappan S. Phosphorylation and function of cardiac myosin binding protein-C in health and disease. *J Mol Cell Cardiol* 2010;**48**:866–875.
23. Marston S, Copeland O, Jacques A, Livesey K, Tsang V, McKenna WJ, Jalilzadeh S, Carballo S, Redwood C, Watkins H. Evidence from human myectomy samples that MYBPC3 mutations cause hypertrophic cardiomyopathy through haploinsufficiency. *Circ Res* 2009;**105**:219–222.
24. Michels M, Soliman OI, Phefferkorn J, Hoedemaekers YM, Kofflard MJ, Dooijes D, Majoor-Krakauer D, Ten Cate FJ. Disease penetrance and risk stratification for sudden cardiac death in asymptomatic hypertrophic cardiomyopathy mutation carriers. *Eur Heart J* 2009;**30**:2593–2596.
25. Pezzoli L, Sana ME, Ferrazzi P, Iascone M. A new mutational mechanism for hypertrophic cardiomyopathy. *Gene* 2012;**507**:165–169.
26. Barefield D, Kumar M, Gorham J, Seidman JG, Seidman CE, de Tombe PP, Sadayappan S. Haploinsufficiency of MYBPC3 exacerbates the development of hypertrophic cardiomyopathy in heterozygous mice. *J Mol Cell Cardiol* 2015;**79**:234–243.

27. Spudich JA. Hypertrophic and dilated cardiomyopathy: four decades of basic research on muscle lead to potential therapeutic approaches to these devastating genetic diseases. *Biophys J* 2014;**106**:1236–1249.
28. van Dijk SJ, Dooijes D, dos Remedios C, Michels M, Lamers JM, Winegrad S, Schlossarek S, Carrier L, ten Cate FJ, Stienen GJ, van der Velden J. Cardiac myosin-binding protein C mutations and hypertrophic cardiomyopathy: haploinsufficiency, deranged phosphorylation, and cardiomyocyte dysfunction. *Circulation* 2009;**119**: 1473–1483.
29. Page SP, Kounas S, Syrris P, Christiansen M, Frank-Hansen R, Andersen PS, Elliott PM, McKenna WJ. Cardiac myosin binding protein-C mutations in families with hypertrophic cardiomyopathy: disease expression in relation to age, gender, and long term outcome. *Circ Cardiovasc Genet* 2012;**5**:156–166.
30. Blankenburg R, Hackert K, Wurster S, Deenen R, Seidman JG, Seidman CE, Lohse MJ, Schmitt JP. Beta-Myosin heavy chain variant Val606Met causes very mild hypertrophic cardiomyopathy in mice, but exacerbates HCM phenotypes in mice carrying other HCM mutations. *Circ Res* 2014;**115**:227–237.
31. Tardiff JC, Carrier L, Bers DM, Poggesi C, Ferrantini C, Coppini R, Maier LS, Ashrafian H, Huke S, van der Velden J. Targets for therapy in sarcomeric cardiomyopathies. *Cardiovasc Res* 2015;**105**:457–470.
32. van der Velden J, Ho CY, Tardiff JC, Olivotto I, Knollmann BC, Carrier L. Research priorities in sarcomeric cardiomyopathies. *Cardiovasc Res* 2015;**105**:449–456.
33. Sakthivel S, Waldmuller S, Saadi AV, Joseph PK, Rakesh PG, Padmakumar R, Tharakan JM, Richard P, Schwartz K, Rajamanickam C, Vosberg HP. Novel mutations in MYH7 and MYBPC3 of an Indian family causing hypertrophic cardiomyopathy. *J Mol Cell Cardiol* 2001;**33**:A105 (abstract).
34. Waldmuller S, Sakthivel S, Saadi AV, Selignow C, Rakesh PG, Golubenko M, Joseph PK, Padmakumar R, Richard P, Schwartz K, Tharakan JM, Rajamanickam C, Vosberg HP. Novel deletions in MYH7 and MYBPC3 identified in Indian families with familial hypertrophic cardiomyopathy. *J Mol Cell Cardiol* 2003;**35**:623–636.
35. Simonson TS, Zhang Y, Huff CD, Xing J, Watkins WS, Witherspoon DJ, Woodward SR, Jorde LB. Limited distribution of a cardiomyopathy-associated variant in India. *Ann Hum Genet* 2010;**74**:184–188.
36. Srivastava A, Garg N, Mittal T, Khanna R, Gupta S, Seth PK, Mittal B. Association of 25 bp deletion in MYBPC3 gene with left ventricle dysfunction in coronary artery disease patients. *PLoS One* 2011;**6**:e24123.
37. Kuster DW, Govindan S, Springer TI, Martin JL, Finley NL, Sadayappan S. A hypertrophic cardiomyopathy-associated MYBPC3 mutation common in populations of South Asian descent causes contractile dysfunction. *J Biol Chem* 2015;**290**:5855–5867.
38. Viswanathan SK, Puckelwartz MJ, Mehta A, Ramachandra CJA, Jagadeesan A, Fritsche-Danielson R, Bhat RV, Wong P, Kandoi S, Schwanekamp JA, Kuffel G, Pesce LL, Zilliox MJ, Durai UNB, Verma RS, Molokie RE, Suresh DP, Khoury PR, Thomas A, Sanagala T, Tang HC, Becker RC, Knoll R, Shim W, McNally EM, Sadayappan S. Association of cardiomyopathy with MYBPC3 D389V and MYBPC3Δ25bp intronic deletion in South Asian descendants. *JAMA Cardiol* 2018;**3**:481–488.
39. Barefield D, Kumar M, de Tombe PP, Sadayappan S. Contractile dysfunction in a mouse model expressing a heterozygous MYBPC3 mutation associated with hypertrophic cardiomyopathy. *Am J Physiol Heart Circ Physiol* 2014;**306**:H807–H815.
40. Lynch TL, Sivaguru M, Velayutham M, Cardounel AJ, Michels M, Barefield D, Govindan S, dos Remedios C, van der Velden J, Sadayappan S. Oxidative stress in dilated cardiomyopathy caused by MYBPC3 mutation. *Oxid Med Cell Longev* 2015; **2015**:424751.
41. Sivaguru M, Fried G, Sivaguru BS, Sivaguru VA, Lu X, Choi KH, Saif MT, Lin B, Sadayappan S. Cardiac muscle organization revealed in 3-D by imaging whole-mount mouse hearts using two-photon fluorescence and confocal microscopy. *Biotechniques* 2015;**59**:295–308.
42. Kumar M, Govindan S, Zhang M, Khairallah RJ, Martin JL, Sadayappan S, de Tombe PP. Cardiac myosin-binding protein C and troponin-I phosphorylation independently modulate myofilament length-dependent activation. *J Biol Chem* 2015;**290**: 29241–29249.
43. Schneider CA, Rasband WS, Eliceiri KW. NIH Image to ImageJ: 25 years of image analysis. *Nat Methods* 2012;**9**:671–675.
44. Rundell VL, Manaves V, Martin AF, de Tombe PP. Impact of beta-myosin heavy chain isoform expression on cross-bridge cycling kinetics. *Am J Physiol Heart Circ Physiol* 2005;**288**:H896–H903.
45. Chandra M, Rundell VL, Tardiff JC, Leinwand LA, De Tombe PP, Solaro RJ. Ca(2+) activation of myofilaments from transgenic mouse hearts expressing R92Q mutant cardiac troponin T. *Am J Physiol Heart Circ Physiol* 2001;**280**:H705–H713.
46. Sumandea MP, Pyle WG, Kobayashi T, de Tombe PP, Solaro RJ. Identification of a functionally critical protein kinase C phosphorylation residue of cardiac troponin T. *J Biol Chem* 2003;**278**:35135–35144.
47. Schlossarek S, Mearini G, Carrier L. Cardiac myosin-binding protein C in hypertrophic cardiomyopathy: mechanisms and therapeutic opportunities. *J Mol Cell Cardiol* 2011;**50**:613–620.
48. Moravsky G, Ofek E, Rakowski H, Butany J, Williams L, Ralph-Edwards A, Wintersperger BJ, Crean A. Myocardial fibrosis in hypertrophic cardiomyopathy: accurate reflection of histopathological findings by CMR. *JACC Cardiovasc Imaging* 2013;**6**:587–596.
49. Lynch TLt, Ismahil MA, Jegga AG, Zilliox MJ, Troidl C, Prabhu SD, Sadayappan S. Cardiac inflammation in genetic dilated cardiomyopathy caused by MYBPC3 mutation. *J Mol Cell Cardiol* 2017;**102**:83–93.
50. Moolman JA, Reith S, Uhl K, Bailey S, Gautel M, Jeschke B, Fischer C, Ochs J, McKenna WJ, Klues H, Vosberg HP. A newly created splice donor site in exon 25 of the MyBP-C gene is responsible for inherited hypertrophic cardiomyopathy with incomplete disease penetrance. *Circulation* 2000;**101**:1396–1402.
51. McConnell BK, Jones KA, Fatkin D, Arroyo LH, Lee RT, Aristizabal O, Turnbull DH, Georgakopoulos D, Kass D, Bond M, Niimura H, Schoen FJ, Conner D, Fischman DA, Seidman CE, Seidman JG. Dilated cardiomyopathy in homozygous myosin-binding protein-C mutant mice. *J Clin Invest* 1999;**104**:1771.
52. Harris SP, Bartley CR, Hacker TA, McDonald KS, Douglas PS, Greaser ML, Powers PA, Moss RL. Hypertrophic cardiomyopathy in cardiac myosin binding protein-C knockout mice. *Circ Res* 2002;**90**:594–601.
53. Uppaluri CR. Heart disease and its related risk factors in Asian Indians. *Ethn Dis* 2002; **12**:45–53.
54. Jones DA, Gallagher S, Rathod KS, Redwood S, de Belder MA, Mathur A, Timmis AD, Ludman PF, Townend JN, Wragg A. Mortality in South Asians and Caucasians after percutaneous coronary intervention in the United Kingdom: an observational cohort study of 279,256 patients from the BCIS (British Cardiovascular Intervention Society) National Database. *JACC Cardiovasc Interv* 2014;**7**:362–371.
55. Maron BJ, Kalra A. Hypertrophic cardiomyopathy in the developing world: focus on India. *Eur Heart J* 2014;**35**:2492–2495.
56. Sadayappan S, Gulick J, Osinska H, Martin LA, Hahn HS, Dorn GW 2nd, Klevitsky R, Seidman CE, Seidman JG, Robbins J. Cardiac myosin-binding protein-C phosphorylation and cardiac function. *Circ Res* 2005;**97**:1156–1163.
57. Sadayappan S, Osinska H, Klevitsky R, Lorenz JN, Sargent M, Molkentin JD, Seidman CE, Seidman JG, Robbins J. Cardiac myosin binding protein C phosphorylation is cardioprotective. *Proc Natl Acad Sci USA* 2006;**103**:16918–16923.
58. Fraysse B, Weinberger F, Bardswell SC, Cuello F, Vignier N, Geertz B, Starbatty J, Kramer E, Coirault C, Eschenhagen T, Kentish JC, Avkiran M, Carrier L. Increased myofilament Ca2+ sensitivity and diastolic dysfunction as early consequences of Mybpc3 mutation in heterozygous knock-in mice. *J Mol Cell Cardiol* 2012;**52**: 1299–1307.
59. Najafi A, Sequeira V, Helmes M, Bollen IA, Goebel M, Regan JA, Carrier L, Kuster DW, Van Der Velden J. Selective phosphorylation of PKA targets after beta-adrenergic receptor stimulation impairs myofilament function in Mybpc3-targeted HCM mouse model. *Cardiovasc Res* 2016;**110**:200–214.
60. Sequeira V, Wijnker PJ, Nijenkamp LL, Kuster DW, Najafi A, Witjas-Paalberends ER, Regan JA, Boontje N, Ten Cate FJ, Germans T, Carrier L, Sadayappan S, van Slegtenhorst MA, Zaremba R, Foster DB, Murphy AM, Poggesi C, Dos Remedios C, Stienen GJ, Ho CY, Michels M, van der Velden J. Perturbed length-dependent activation in human hypertrophic cardiomyopathy with missense sarcomeric gene mutations. *Circ Res* 2013;**112**:1491–1505.
61. McNamara JW, Li A, Smith NJ, Lal S, Graham RM, Kooiker KB, van Dijk SJ, Remedios CGD, Harris SP, Cooke R. Ablation of cardiac myosin binding protein-C disrupts the super-relaxed state of myosin in murine cardiomyocytes. *J Mol Cell Cardiol* 2016;**94**:65–71.
62. McNamara JW, Li A, Lal S, Bos JM, Harris SP, van der Velden J, Ackerman MJ, Cooke R, Dos Remedios CG. MYBPC3 mutations are associated with a reduced super-relaxed state in patients with hypertrophic cardiomyopathy. *PLoS One* 2017;**12**: e0180064.
63. Toepfer CN, Wakimoto H, Garfinkel AC, McDonough B, Liao D, Jiang J, Tai AC, Gorham JM, Lunde IG, Lun M, Lynch TL, McNamara JW, Sadayappan S, Redwood CS, Watkins HC, Seidman JG, Seidman CE. Hypertrophic cardiomyopathy mutations in MYBPC3 dysregulate myosin. *Sci Transl Med* 2019;**11**.pii:eaat1199.
64. Schlossarek S, Frey N, Carrier L. Ubiquitin-proteasome system and hereditary cardiomyopathies. *J Mol Cell Cardiol* 2014;**71**:25–31.